NON-LINEAR PROPAGATION OF ELASTO-PLASTIC WAVES IN RODS
- A comparison with experimental results -

R. Rittel, Rheinmetall GmbH, Ulmenstrasse 125
D-4000 Düsseldorf, W-Germany

The investigation of elasto-plastic material behaviour of rigid bodies at extremly short loadings was not to measure exactly for a long time. For various applications e.g. simulation of car-crash, impact of meteorites, terminal ballistic problems etc. the knowledge of the dynamic behaviour of materials is necessary. G. KUSCHER from the Ernst-Mach-Institute, W-Germany, carried out the first time experiments that allow the examination of the elasto-plastic theory of wave propagation in rods. This report presents computational studies on non-linear propagation of elasto-plastic waves in rods, that were carried out with the MSC-PISCES-Code, and the comparison to experimental results which lead to a deeper insight into and, in connection with computational graphics, to a better visualization in material behaviour.

1. Introduction

The investigation of elastic-plastic behaviour of materials of rigid bodies at extremly short loadings can only be measured with measuring techniques which are able to record such processes continuously with sufficiently small time steps. At the Ernst-Mach-Institute, W-Germany, this was realized under use of laser in the interferometrie. The motion of faces of rigid bodies could be measured in the region of nanoseconds. This new measuring technique called VISAR (Velocity Interferometer System for Any Reflector) /1/ offers the additional advantage that the values can be measured without any contact.
The investigations are carried out with rods of different materials which were loaded by cylindrical plates of different velocities. Due to impact velocity, the density of the material of the rod and the dynamic yield stress of this material, an elastic or an elasto-plastic reaction of the material can be realized.

Out of a lot of experiments are those considered which were carried out by use of rods out of the tungsten sinter alloy D17. The chosen experiments are calculated with the 2-dimensional MSC-PISCES-code. Here the results of the computational work are shown in comparison to the theory and the experiments.

2. Theory

The theoretical derivation of non-linear propagation of elasto-plastic waves in rods is published by several authors such as VON KARMAN /2/, RAKHMATULIN /3/ and TAYLOR /4/. At this point only the occuring phenomena are shortly described.
The steel plate impacts the rod. A compression wave with amplitudes which yield in stresses higher than the dynamic yield stress determines the elasto-plastic two-wave structure. The elastic wave loads the material up to the dynamic yield stress and runs through the material with the sound speed of the unloaded material. The plastic deformation wave follows the elastic wave with a lower non-linear velocity. The elastic wave is reflected at the rear of the rod, and, after running back, at the elasto-plastic boundary. This process repeats several times. The time between two successive reflections at the rear of the rod respectively at the elasto-plastic boundary becomes shorter because of the moving elasto-plastic boundary. Each reflection of the elastic wave at the rear of the rod results in an acceleration of the rear. The time period between the reflections of the elastic wave the material lying between the rear of the rod and the elastic wave is unloaded, the velocity remains constant.
One of the fundamental ideas of the elasto-plastic theory is the ascertainment that the elastic wave loads the material just up to the dynamic yield stress. Thus it is possible to calculate the dynamic yield stress out of the measured change in velocity by

$Y = 0.5 * \Delta V * \rho * C_o$ with

Y - dynamic yield stress
ΔV - change in velocity
ρ - material density
C_o - initial sound speed

The dynamic yield stress is independent of the impact velocity and the geometry of the rods.

3. Experimental device

The mechanical part of the test device can be seen in Figure 1. Details to the test device can be read in /1/. The steel plate with a diameter of 40 mm and a thickness of 15 mm was attached to a plastic sabot and was driven by a propelling charge. The plate velocity was measured by two gauges. The plate impacts the stationary specimen. The rear velocity of the rod was measured by the use of laser. The amount of the whole accelerated mass (steel plate plus sabot) was 250 g. All specimen had a diameter of 5.8 mm and a length to diameter ratio of 10.

4. Numerical modelling

The calculations were carried out with the 2-dimensional MSC-PISCES-code on a VAX 8700 - computer. The structure is shown in Figure 2. The geometry is axially symmetric. Since the deformation of the rod and the steel plate was expected to be small, both subgrids were modelled in Lagrangian coordinates. A few calculations with different numbers of cells have shown that the discretisation with 205 cells for the rod was sufficient. To yield the same mass as the whole accelerated mass in experiments, the plate thickness was expanded.
The initial condition for the plate was the respective velocity. The interaction between both meshes was realized by use of the impact logic. The impact logic tests points of a polygon around a mesh for impacts with other polygons and resets them to the surface of the polygon in several time steps by applying a force to the nodes which are inside the polygon. This impact logic was used on both polygons, the rod and the plate, to get a smoother interaction. Between the polygons no friction was used.
Dependent on the impact velocity up to 5 rezoning steps were necessary because of the deformation of the nose of the rod at the impact boundary.

5. Material models

For both materials, steel and tungsten alloy, elastic - perfectly plastic material models were used. The main parameters of these models are

- Steel	density	-	7865	[kg/m³]
	bulk modulus	-	1.69E11	[Pa]
	shear modulus	-	7.90E10	[Pa]
	dynamic yield stress	-	1.20E9	[Pa]
- Tungsten	density	-	17000	[kg/m³]
	bulk modulus	-	3.13E11	[Pa]
	shear modulus	-	1.61E11	[Pa]
	dynamic yield stress	-	1.30E9	[Pa]

The dynamic yield stress of the tungsten alloy was calculated out of the experiments described in /1/. The static stress-strain curve is shown in the Figure beneath the text. The static yield stress is nearly the half of the dynamic yield stress.

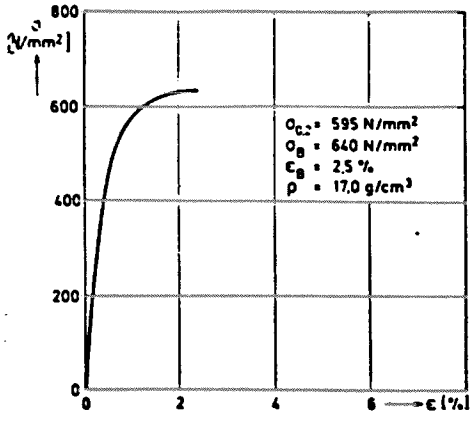

Stress-strain curve for Tungsten alloy D17

6. Comparison of the results

The calculations were carried out with three impact velocities. The theoretical predicted velocity curve in form of steps is shown in Figure 4 and, for a time period near the first reflection of the pressure wave, in Figure 7 on the left side of the bottom.

The resulting velocity curves agree well with the corresponding experimental curves (Figure 3). The increase in velocity was measured to 30.6 m/s + 5 % opposite to 32 m/s reached in the computersimulation.
Figures 5 and 6 are showing the moving pressure wave with a maximum of 400 MPa at times near the first reflection of the pressure wave at the rear of the rod and the equivalent stress caused by the pressure. The maximum equivalent stress reaches the value of the dynamic yield stress (see also Figure 7 on the right side of the top).
Time histories near the rear of the rod for a time period up to 30 μs is shown in Figure 7. Between two successive reflections of the pressure wave the material is unloaded, that means the velocity between two reflections remain constant. This agrees with the elasto-plastic theory.
The velocity curve with an impact velocity of 388 m/s and the belonging accelerations can be seen in Figure 8. Figure 9 and 10 compare the accelerations with impact velocities of 240 m/s and 579 m/s. The agreement could be seen to be qualitatively good. Differences occuring in the maximum values of the acceleration are resulting from the time step which was 10 times smaller during the calculations.
The proceeding of elasto-plastic waves can be shown meaningful by use of Lagrange-diagrams. Figure 11 shows the Lagrange-diagram for the experimental results whereas the corresponding one for the computational results can be seen in Figure 12. They agree well with differences of 3 mm in the final length and 2 mm in the width of the plastic deformation zone. The line showing the zone of plastic deformation is non-linear, thus the velocity of the plastic front is non-linear.
Figure 13 shows two velocity curves, both were calculated with an impact velocity of 388 m/s. The dynamic yield stress varied. The increase in velocity can be seen to be direct proportional to the dynamic yield stress. Also the maximum pressure, equivalent stress, stress deviator and stress tensor are direct proportional. It can't be found any fact that can be a reason for failure of rods whereas in experiments rods with high dynamic yield stresses are broken shortly after the first reflection of the pressure wave. To find failure criteria this work is still in progress.

7. Conclusions

The elasto-plastic theory was confirmed by experiments and also by calculations with the MSC-PISCES-code. The theoretical predicted velocity curves of the rear of a rod in form of steps introduced by the reflexions of the elastic pressure wave could be measured and can be seen in the numerical calculations. We realize that, as VON KARMAN predicted, the change of velocity of the rear of a rod out of one material is constant and independent of impact velocity and geometry of the rod. The non-linear velocity curve of the elasto-plastic boundary could be proved with a good agreement between experiment and calculation.
An increase of the static yield stress, thus also an increase of the dynamic yield stress, leads to higher velocity changes and is direct proportional to the increase in yield stress. In the experiments it could be realized a failure of rods out of materials with high yield stresses. To find a failure criteria, necessary for the design of KE-penetrators that are produced in our house, this work is still in progress.

References

/1/ G. KUSCHER
Nicht-lineare Ausbreitung elasto-plastischer Wellen in KE-Penetratoren, (1985)

/2/ VON KARMAN T., DUWEZ, P.
J.Appl.Phys. 21, 987 (1950)

/3/ RAKHMATULIN K.A.
Appl.Math. and Mech., 9, No. 1 (1945)

/4/ TAYLOR G.I.
J.Inst.Civ.Eng. 26, 486 (1946)

/5/ HANCOCK S.L.
Finite Difference Equations for PISCES 2DELK
Phys. Intern. Comp., Report TCAM-76-2, 1976

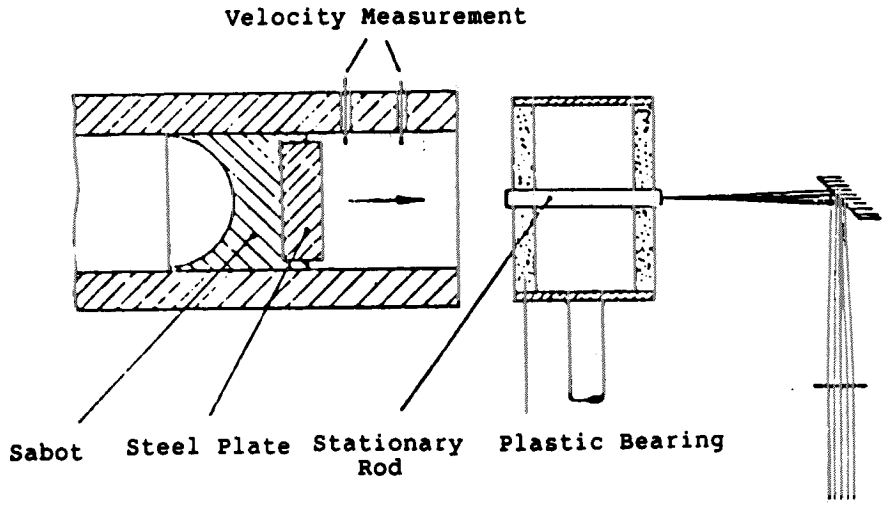

Figure 1: EXPERIMENTAL DEVICE

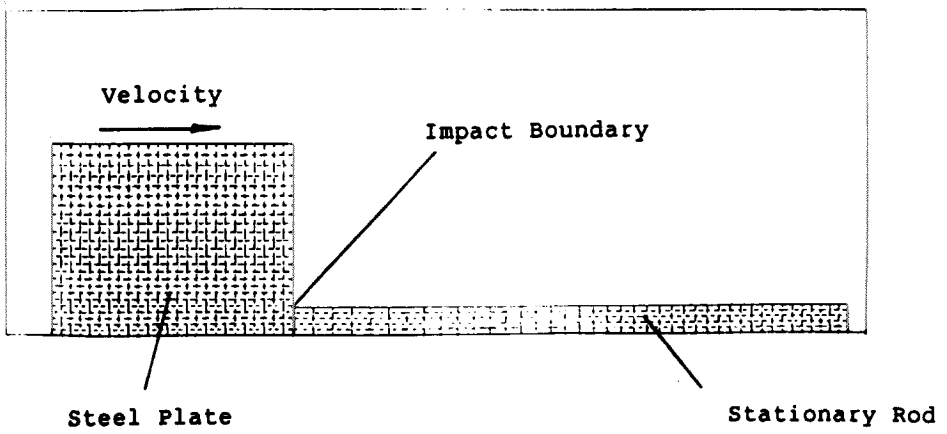

Figure 2: MESHES FOR COMPUTERSIMULATION

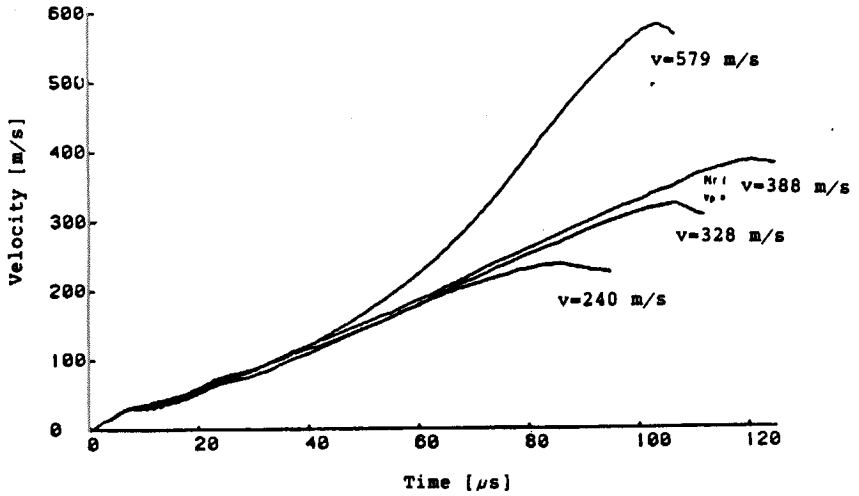

Figure 3: VELOCITY CURVES (EXPERIMENT)

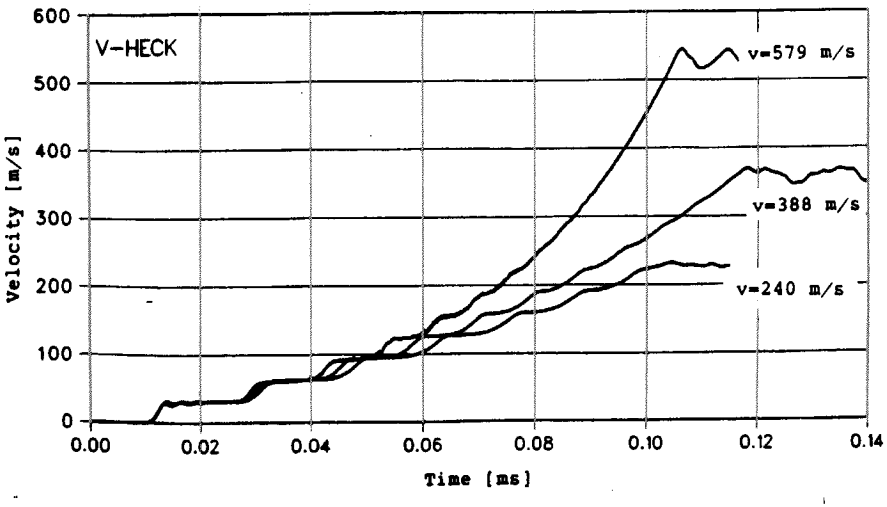

Figure 4: VELOCITY CURVES (COMPUTERSIMULATION)

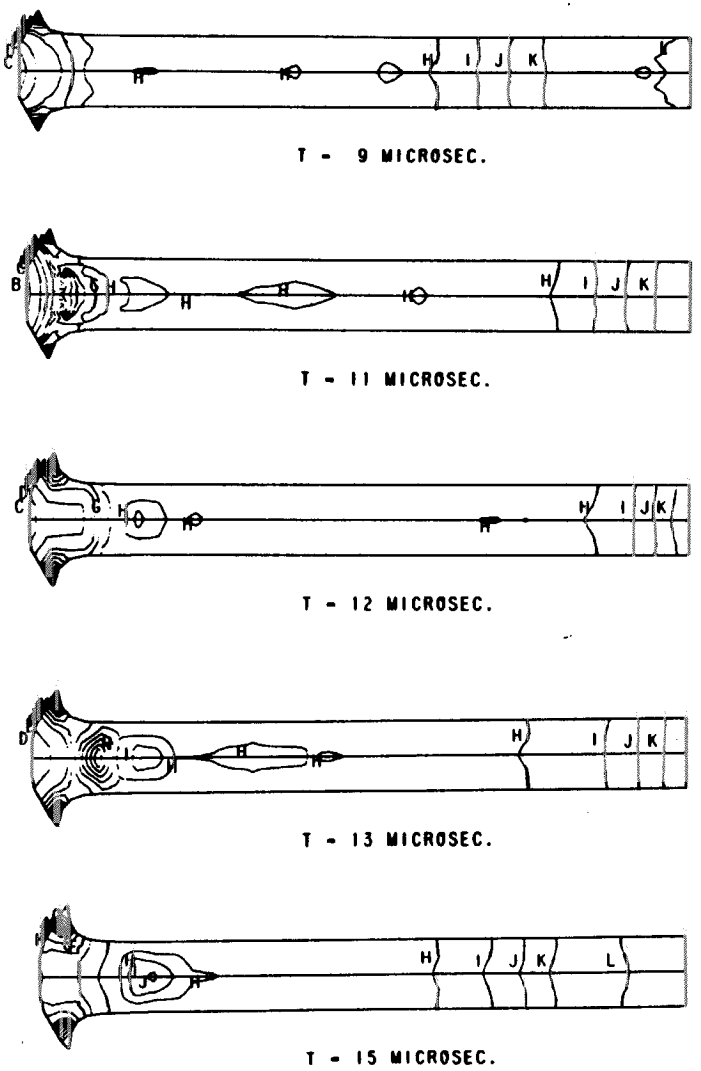

Pressure [MPa]

A = 4000
B = 3000
C = 2000
D = 1500
E = 1000
F = 800
G = 600
H = 400
I = 300
J = 200
K = 100
L = -100

Figure 5: PRESSURE WAVE (FIRST REFLECTION)

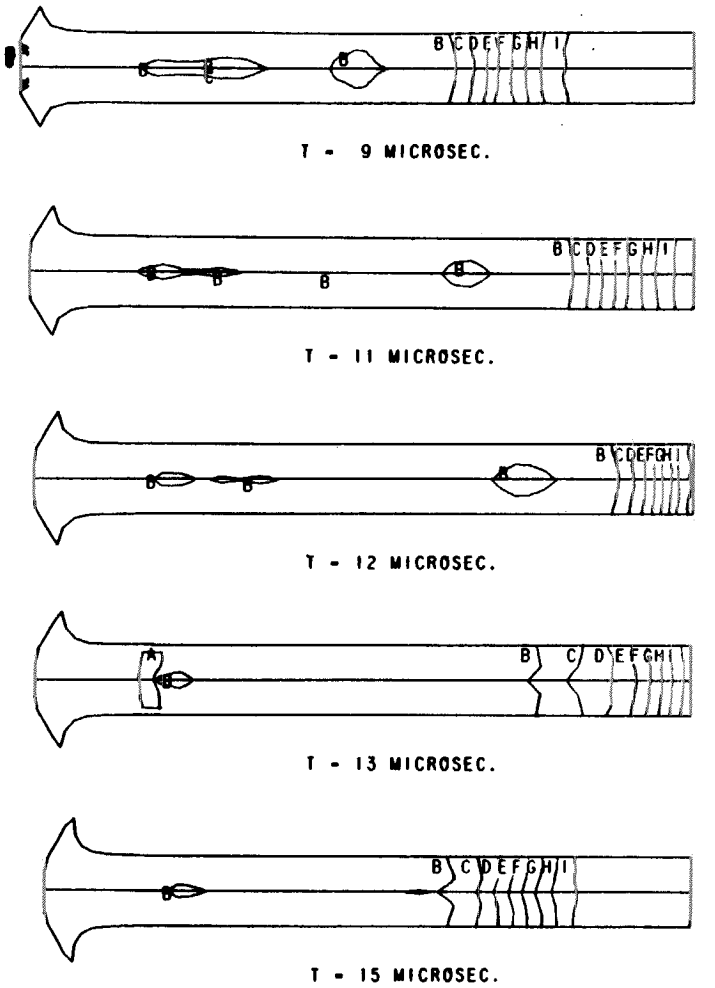

Equiv. Stress [MPa]

A = 1350
B = 1200
C = 1050
D = 900
E = 750
F = 600
G = 450
H = 300
I = 150
J = 0

Figure 6: EQUIVALENT STRESS (FIRST REFLECTION)

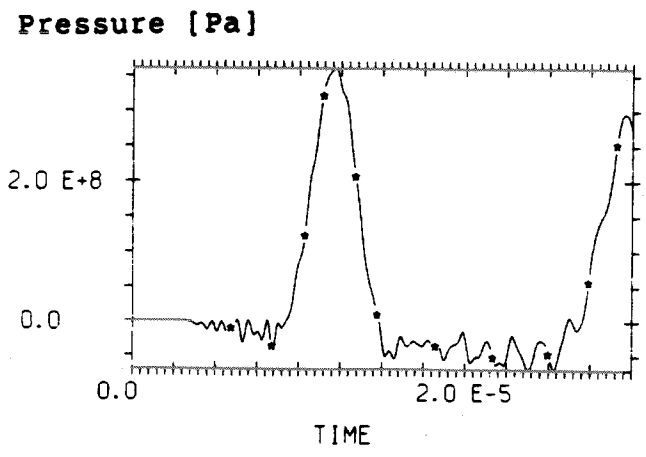

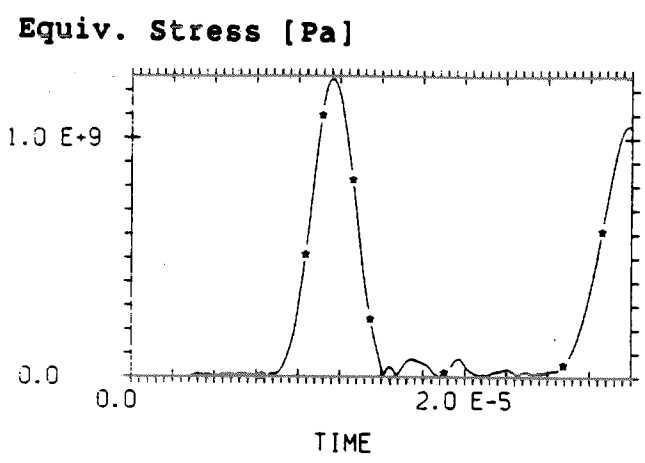

all times in seconds

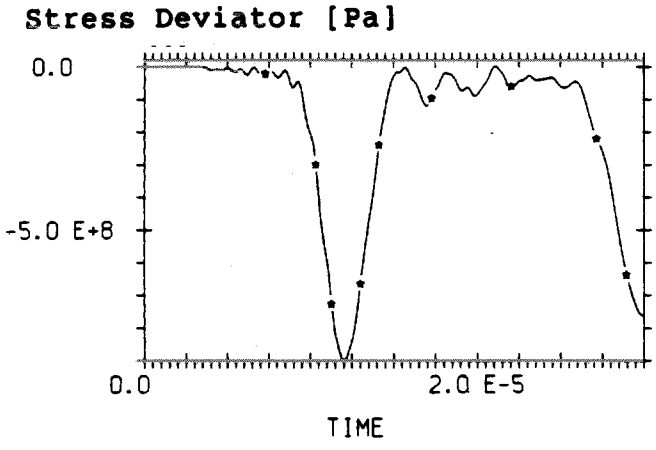

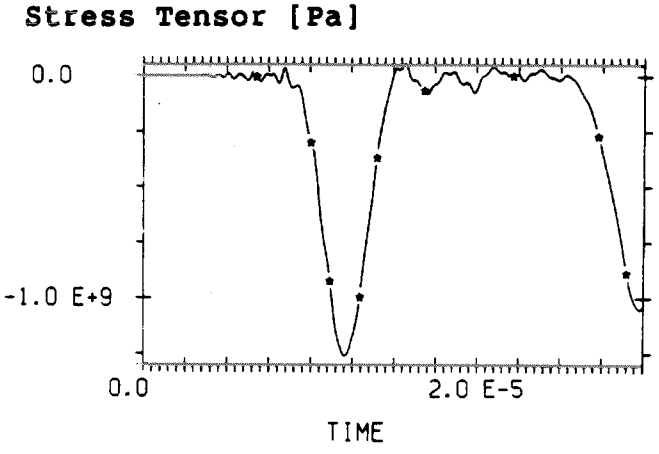

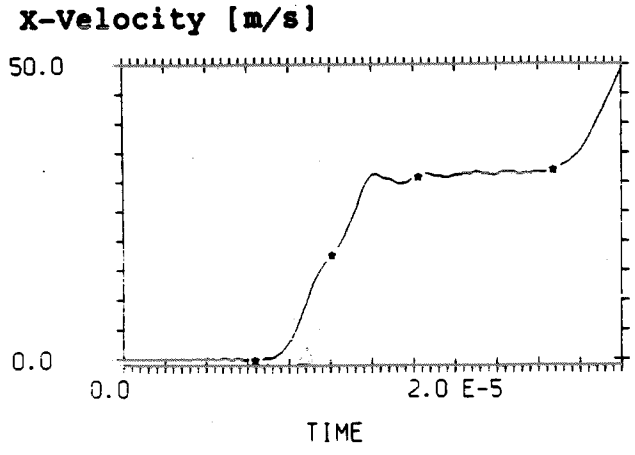

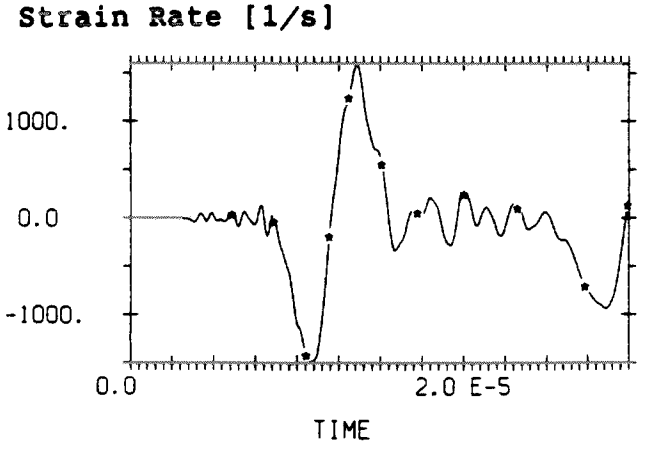

Figure 7: TIME HISTORIES NEAR THE REAR OF THE ROD TIME PERIOD AT THE FIRST REFLECTION

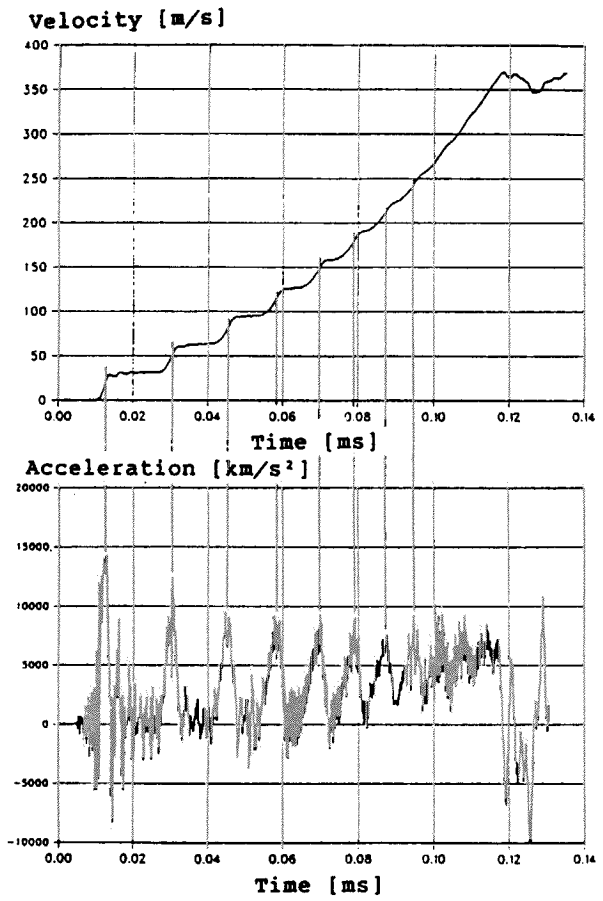

Figure 8:
VELOCITY AND ACCELERATION CURVE
IMPACT VELOCITY V=388 M/S

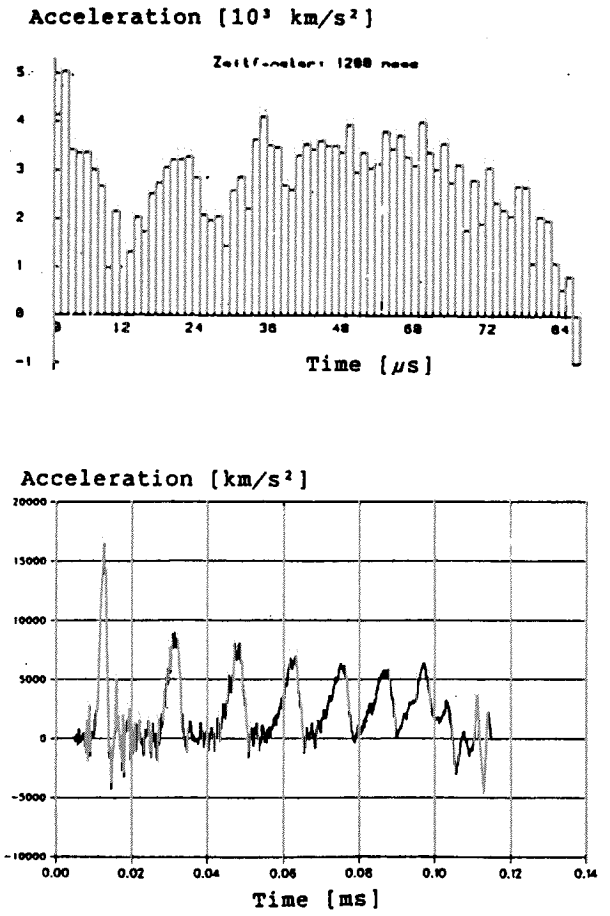

Figure 9:
ACCELERATION CURVES
IMPACT VELOCITY V=240 M/S

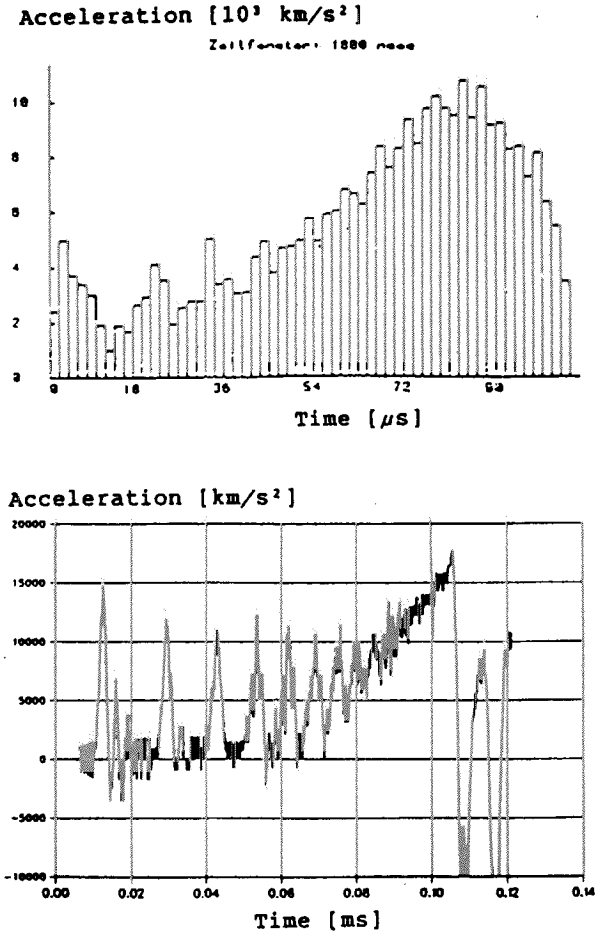

Figure 10:
ACCELERATION CURVES
IMPACT VELOCITY V=579 M/S

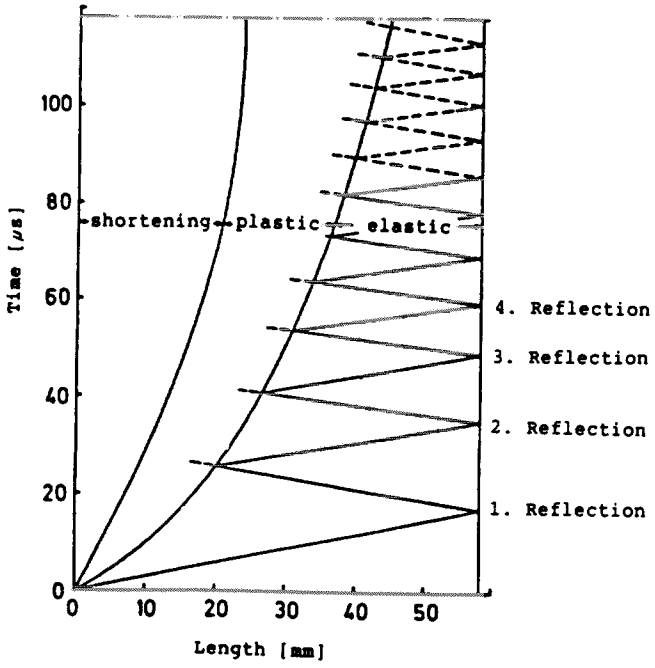

Figure 11:
LAGRANGE DIAGRAM, EXPERIMENT
IMPACT VELOCITY V=388 M/S

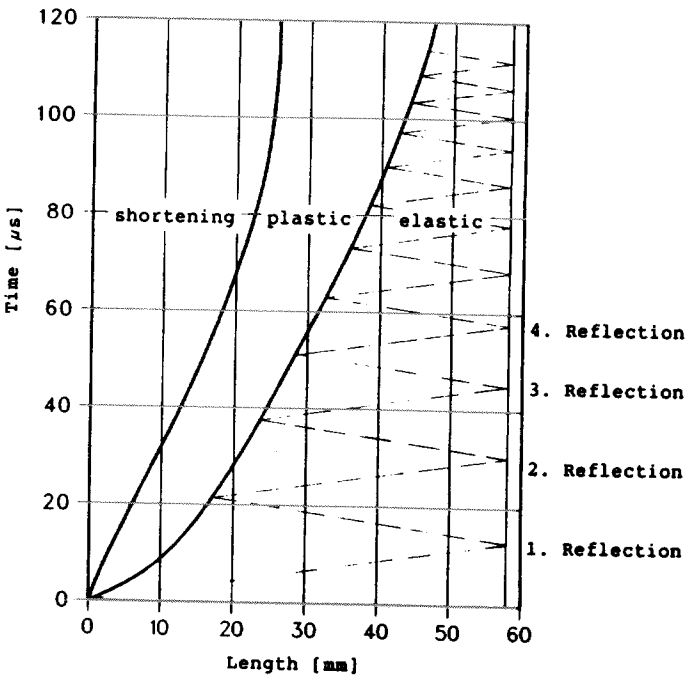

Figure 12:
LAGRANGE DIAGRAM, COMPUTERSIMULATION
IMPACT VELOCITY V=388 M/S

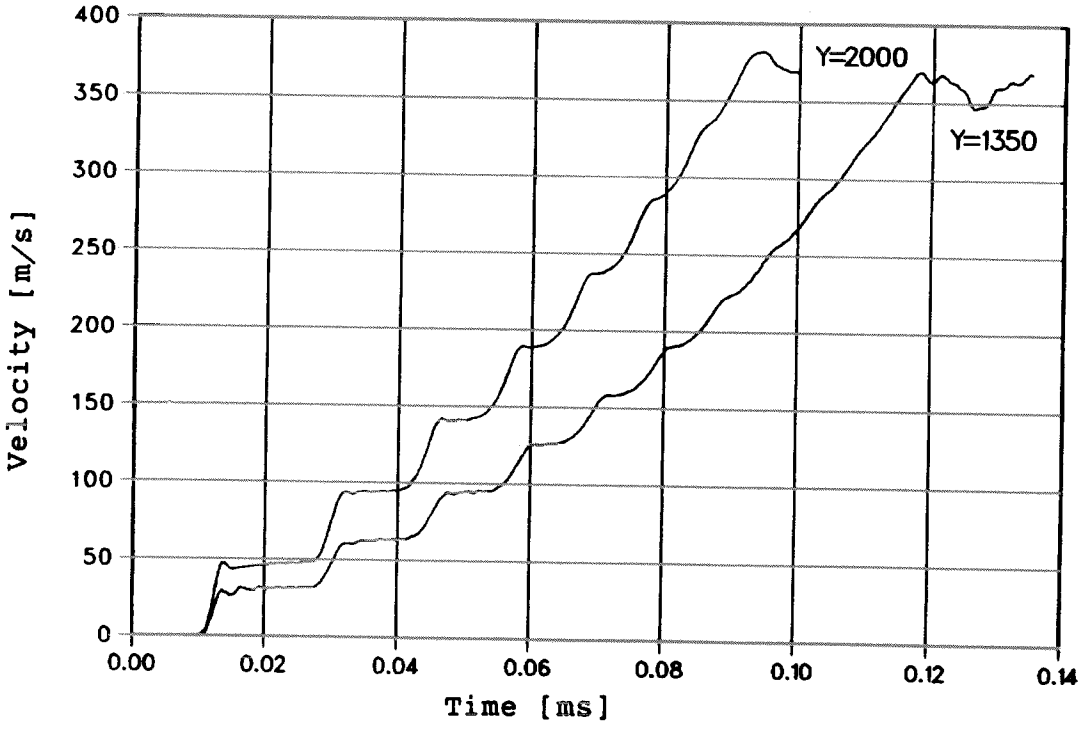

Figure 13:
VELOCITY CURVES, INFLUENCE OF THE DYNAMIC YIELD STRESS
IMPACT VELOCITY V=388 M/S